Characterization of an organic semiconductor diode for dosimetry in radiotherapy

Characterization of an organic semiconductor diode for dosimetry in radiotherapy

Jessie A. Posar, Jeremy Davis, and Matthew J. Large
Centre for Medical Radiation Physics, University of Wollongong, Wollongong, NSW 2522, Australia

Laura Basiricò, Andrea Ciavatti, and Beatrice Fraboni
Department of Physics and Astronomy, University of Bologna, Viale Berti Pichat 6/2, Bologna 40127, Italy

Olivier Dhez
ISORG, 60 Rue des berges, Parc Polyetc, Immeuble Tramontane, Grenoble 38000, France

Dean Wilkinson
Centre for Medical Radiation Physics, University of Wollongong, Wollongong, NSW 2522, Australia
Illawarra Cancer Care Centre, Wollongong Hospital, Wollongong, NSW 2500, Australia

Paul J. Sellin
Department of Physics, University of Surrey, Guildford, Surrey GU2 7XH, UK

Matthew J. Griffith
Priority Research Centre for Organic Electronics, University of Newcastle, Callaghan, NSW 2308, Australia
School of Aeronautical, Mechanical and Mechatronic Engineering, University of Sydney, Camperdown, NSW 2050, Australia

Michael L. F. Lerch, Anatoly Rosenfeld, and Marco Petasecca[a)]
Centre for Medical Radiation Physics, University of Wollongong, Wollongong, NSW 2522, Australia

(Received 5 March 2020; revised 15 April 2020; accepted for publication 1 May 2020; published xx xxxx xxxx)

Purpose: The development of novel detectors for dosimetry in advanced radiotherapy modalities requires materials that have a water equivalent response to ionizing radiation such that characterization of radiation beams can be performed without the need for complex calibration procedures and correction factors. Organic semiconductors are potentially an ideal technology in fabricating devices for dosimetry due to tissue equivalence, mechanical flexibility, and relatively cheap manufacturing cost. The response of a commercial organic photodetector (OPD), coupled to a plastic scintillator, to ionizing radiation from a linear accelerator and orthovoltage x-ray tube has been characterized to assess its potential as a dosimeter for radiotherapy. The radiation hardness of the OPD has also been investigated to demonstrate its longevity for such applications.

Methods: Radiation hardness measurements were achieved by observing the response of the OPD to the visible spectrum and 70 keV x rays after pre-exposure to 40 kGy of ionizing radiation. The response of a preirradiated OPD to 6-MV photons from a linear accelerator in reference conditions was compared to a nonirradiated OPD with respect to direct and indirect (RP400 plastic scintillator) detection mechanisms. Dose rate dependence of the OPD was measured by varying the surface-to-source distance between 90 and 300 cm. Energy dependence was characterized from 29.5 to 129 keV with an x-ray tube. The percentage depth dose (PDD) curves were measured from 0.5 to 20 cm and compared to an ionization chamber.

Results: The OPD sensitivity to visible light showed substantial degradation of the broad 450 to 600 nm peak from the donor after irradiation to 40 kGy. After irradiation, the spectral shape has a dominant absorbance peak at 370 nm, as the acceptor better withstood radiation damage. Its response to x rays stabilized to 30% after 35 kGy, with a 0.5% difference between 770 Gy increments. The OPD exhibited reproducible detection of ionizing radiation when coupled with a scintillator. Indirect detection showed a linear response from 25 to 500 cGy and constant response to dose rates from 0.31 Gy/pulse to 3.4×10^{-4} Gy/pulse. However, without the scintillator, response increased by 100% at low dose rates. Energy independence between 100 keV and 1.2 MeV advocates their use as a dosimeter without beam correction factors. A dependence on the scintillator thickness used during a comparison of the PDD to the ionizing chamber was identified. A 1-mm-thick scintillator coupled with the OPD demonstrated the best agreement of $\pm$ 3%.

Conclusions: The response of OPDs to ionizing radiation has been characterized, showing promising use as a dosimeter when coupled with a plastic scintillator. The mechanisms of charge transport and trapping within organic materials varies for visible and ionizing radiation, due to differing properties for direct and indirect detection mechanisms and observing a substantial decrease in sensitivity to the visible spectrum after 40 kGy. This study proved that OPDs produce a stable response to

6-MV photons, and with a deeper understanding of the charge transport mechanisms due to exposure to ionizing radiation, they are promising candidates as the first flexible, water equivalent, real-time dosimeter. © *2020 American Association of Physicists in Medicine* [https://doi.org/10.1002/mp.14229]

Key words: dosimetry, organic semiconductors, radiotherapy

1. INTRODUCTION

In radiotherapy quality assurance (QA), the development of novel materials and devices that can provide accurate monitoring of the amount of energy absorbed in the desired material with instant feedback, precise spatial resolution, and mechanical flexibility remains a substantial unsolved challenge.[1] The over-response of common commercially available inorganic, solid-state devices, that is, silicon diodes, requires complex calibration procedures to match the absorbed dose in water.[2] Therefore, research has branched out to investigate a range of devices and materials that can overcome these limitations and provide a solution. Within the field of solid-state devices, diamond is an ideal candidate as a replacement for silicon due to its near tissue equivalence as a result of its carbon composition,[3,4] radiation hardness,[5] and near energy independence for x rays[6] and heavy charged particles.[7,8] However, the energy necessary to create electron-hole pairs in diamond is very high (13 eV), reducing their sensitivity to lower energy events.[9] Furthermore, fabrication of diamond detectors is expensive due to the low yield of production and response reproducibility. Single-crystal diamond substrates are limited to lateral dimensions $<9\times9$ mm^2, leading to expensive mosaic detectors that limit their compatibility with scaled-up fabrication processes.[10,11] The PTW microDiamond is currently the only commercial diamond-based detector being considered for a range of radiation therapy applications due to its high spatial resolution (1-μm-thick sensitive volume[12]) when operated in edge-on mode[13] and capability to perform dosimetry in real time.[14] However, in small field dosimetry, the PTW microDiamond over responds in fields smaller than 20mm compared to other detectors due to the perturbation created by extra cameral materials such as the electrodes.[15]

Radiographic film dosimetry is achieved by film polymers changing optical density due to the interaction with radiation to provide a latent image. Calibration of the optical density with known delivery of the dose is then required to obtain a quantitative map of the absorbed dose.[16] This method has high two-dimensional spatial resolution and provides simple field mapping. However, film requires a minimum pre-readout wait time of 24 h to allow for stabilization of postirradiation darkening, and its response is dependent on the protocol used, that is, cut margin, calibration area, handling, scanner resolution, and temperature.[17–19] Gel-based dosimetry provides all the advantages of its film-based counterpart, however, it also extends the data acquisition into three dimensions. Similar to film, gel dosimetry uses radiation chromatic material.[20] Like film, gel dosimetry is also time sensitive and labor intensive, requiring immediate access to a medical imaging apparatus, commonly computed tomography (CT) or magnetic resonance imaging (MRI), to obtain the three-dimensional dose distribution. While film and gel have high spatial resolutions, their inability to be used as a real-time dosimeter for *in vivo* applications is an unavoidable issue.

Current tissue-equivalent devices that achieve real-time monitoring are fiber-optic dosimeters. These devices, comprised of a scintillator optically coupled to a photomultiplier tube (PMT) or a silicon-based photodiode via an optical fiber, have been extensively investigated for radiotherapy applications.[21] A plastic scintillator generates light with an intensity that is proportional to the energy deposition of the incident ionizing radiation and travels through an optical fiber to a detector. Fiber optics-based devices are capable of real-time monitoring, and have been described as flexible dosimeters with high spatial resolution due to their small size (from 1-mm to 10-um thick in special applications).[21,22] However, their flexibility is limited by the defined minimal angle a fiber optic can bend without breaking and the scintillator being glued onto the fiber, thus the assembly is relatively rigid. Ideally, all the light from the scintillator would travel down the fiber optic and be detected by a device at a distance away from the radiation source. However, many issues arise from this setup in terms of efficiency, accuracy, and response reproducibility. First, isotropic emission of the scintillation light results in only a fraction of photons traveling toward the fiber optics.[23] The limited quantum efficiency of the scintillator also limits the response, with only a small proportion of energy being absorbed and converted into light. To mitigate these problems, highly reflective materials, that is, polytetrafluoroethylene (Teflon)-based tape and metal-based paint, that is, titanium spray[24] are used to trap the emitted light[21,25], the latter often at the expense of the tissue equivalence of the dosimeter. Also, the three devices used, that is, the scintillator, fiber optic, and detector, require optimal optical coupling to avoid large impact on the light collection efficiency of the system. Finally, light can also be generated by the direct interaction of radiation with the optical fibers, known as Cerenkov radiation, which may not be proportional to dose.[26] While subtraction of this background signal can be achieved, no methodology is accurate enough to entirely remove the effect of Cerenkov radiation. The eventual use of fiber optics in an array for field mapping would also become bulky and expensive due to the need for individual optical fibers for each scintillator, as well as secondary probes for Cerenkov signal subtraction, if required.

Photodetectors based on organic semiconductors have recently gained momentum in the field of radiation detection due to their relatively inexpensive production costs and simple large area printing fabrication techniques.[27–29] Organic materials are an attractive technology for advanced dosimetry applications as they can be read out in real time, like solid-state semiconducting materials, but with the chemical and mechanical benefits of organic compounds such as plastics. Given their low density (1 to 1.3 g/cm^3) and predominantly hydrogen- and carbon-based elemental composition, they have a response to radiation able to mimic that of water. Furthermore, they can be dissolved in solutions to create inks that can be printed onto mechanically flexible substrates with cheap manufacturing processes for the production of large area detectors. Characterization of the charge generation and charge transport in organic materials from ionizing radiation and the effect radiation damage has on these processes is still an ongoing field of research. Dosimeters for medical applications must withstand a minimal radiation dose of 500 Gy/year, with any changes in the response due to radiation damage to be accounted for by correction factors.[30,31] The first study of electron transport variations in electron beam irradiated polyacetylene was performed in 1983.[32] Since then, semiconducting polymers have been used as detectors for a variety of radiation sources.[33,34] Direct x-ray induced photocurrent in conjugated polymers has been achieved with kV x rays in a range of materials including poly[2-methoxy-5-(2'-ethylhexyloxy)-1,4-phenylene vinylene] (MEH-PVV) and poly(9,9-dioctylfluorene) (PFO), with no observed effect on their performance up to an accumulated dose of 10 Gy.[35] Blending conjugated polymers with highly conductive (TIPS)-Pentacene has been shown to increase kV x-ray sensitivity to 457 nC/mGy/cm^3, four times that of pure Poly(triarylamine) (PTAA) material.[36] Research has since then focused on increasing the direct detection sensitivity of organic thin films by combining the active material with high atomic number (Z) nanoparticles (NP) to increase high-energy photon absorption.[37,38] Organic semiconductors blended with bismuth oxide NP were shown to increase sensitivities to 1712 μC/mGy/cm^3 for 50 kV x rays.[39] While using high Z materials increases the photoelectric absorption cross section, this compromises the tissue/water equivalence of the device, which is the main benefit for use in radiotherapy applications. This study focused on the characterization of an organic photodetector (OPD) combined with a plastic scintillator for detection of ionizing radiation for dosimetry applications. Organic photodetectors are constructed of acceptor and donor materials, similar to many solid-state detectors currently available and used in clinical practice.[40] However, unlike their crystalline solid-state counterparts, there is no one distinct junction between the two materials as they are structured as a blended heterojunction. The most common donor material for organic solar cells is the conjugated polymer poly(3-hexylthiophene) (P3HT) blended with fullerene derivative phenyl-C61-butyric acid methyl ester (PCBM) as the acceptor.[41,42] The use of P3HT:PCBM to measure 70 kV x rays has been reported within the context of their exploitation in the field of medical imaging, showing that with the aid of a NaI(Tl) or a CsI(Tl) scintillator the device response is linearly dependent on the x-ray dose rate.[43] This material has also been shown to be sensitive to 6 MV x rays via indirect detection (Gd_2O_2S:Tb phosphor material) with stable performance (2% loss in photocurrent) up to 360 Gy,[44] suggesting its longevity for applications in ionizing radiation environments. Currently, no clinical-based measurements have been carried out to show how the device would perform if used for dosimetry purposes, nor have OPD devices been tested past 500 to 600 Gy of total irradiation doses. Such investigations can be used to determine if organic photodetectors are suitable for use after being exposed to harsh irradiation conditions, and whether correction factors are needed for their use in radiotherapy.

We assessed the potential of thin-film photodetector technology in the area of radiotherapy dose verification. In particular, the response to radiation was characterized under various clinically relevant conditions when preirradiated up to 40 kGy of gamma radiation for investigation of radiation hardness/damage in medical radiation applications.

2. METHODS AND MATERIALS

2.A. Organic photodetector

The OPDs were produced by ISORG (Grenoble — France) and feature a 500-nm-thick bulk heterojunction with an active area of 4.91 mm^2. The basic structure is presented in Fig. 1, consisting of an indium tin oxide (ITO) transparent anode deposited on the top side of the substrate and a back contact attached to a gold pad. The photodetector was covered with a protective film (Polyethylene, 25-μm thick) and mounted onto a Printable Circuit Board (PCB) (FR-4) for ease of connection to the readout electronics via pins 1 and 2. A plastic scintillator (RP400, Rexon), with thicknesses varying between 0.5 and 2 mm, was coupled to the OPD with optical grease (RX-688).

2.B. Radiation hardness study

In the past, radiation damage to plastic scintillators, such as the RP400, has been extensively characterized for high-energy physics applications due to their low cost, mechanical plasticity, and fast decay time. It has been proven that the plastic scintillator RP400, adopted in this work, has a relatively low variation of the light yield due to radiation damage up to 10 kGy (<8%) of accumulated dose by irradiation with a cobalt-60 gamma source.[45,46] So, in order to establish the stability of the combination of an RP400 scintillator with an organic photodetector, we tested the response variation of two OPDs by irradiating them with a cobalt-60 gamma source (dose rate = 1.2 kGy/h) to a total irradiation dose (TID) of 40 kGy. During irradiation, the photodetectors were embedded in a plexiglass holder with a 1.5-cm-thick window between the gamma source and sample surface. Irradiation occurred in five steps from 0.1 to 1 kGy in steps of 0.25 kGy with further larger steps of 10 kGy to reach a

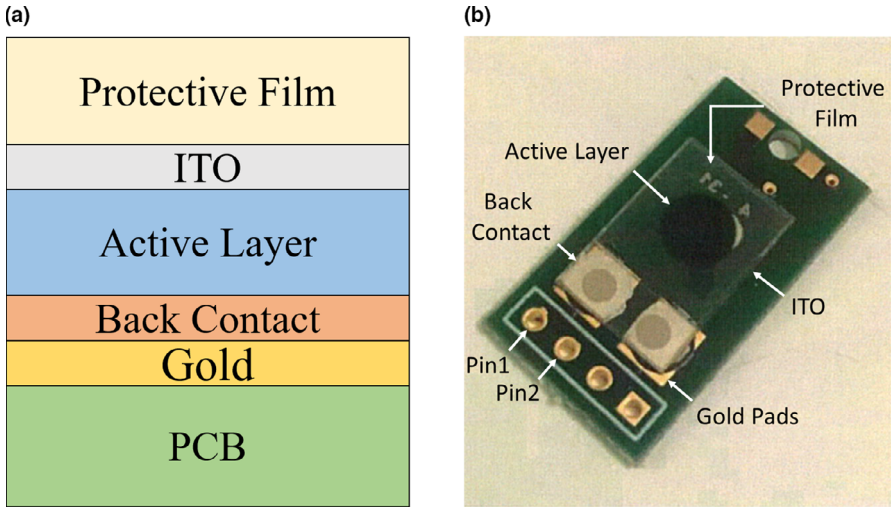

FIG. 1. (a) Cross section (not to scale) and (b) picture of the photodetectors architecture. The 25-μm-thick protective film sits on top of the indium tin oxide transparent contact, attached to the Printable Circuit Board with gold pads.

TID of 40 kGy. The remaining nonirradiated OPDs were used as reference samples. Three characteristic measurements were performed as a function of accumulated radiation exposure. First, the current density-voltage (JV) characteristics were measured using a Picoammeter/Voltage Source (Keithley 487) applying bias from −10 to 2 V, in dark conditions. The second measurement was determination of the UV–Vis photocurrent variation as a function of the wavelength after the TID of 40 kGy. A monochromator (9055F, Sciencetech) was used to step through a range of visible wavelengths from a xenon lamp. The monochromator had a slit aperture of 0.25 mm, allowing for approximately 0.8 nm resolution. Each wavelength was pulsed via a mechanical chopper (SR540) before reaching the tested sample. The photocurrent response from the sample due to the incident wavelength was measured and averaged over multiple pulses. The spectrum was split into two ranges, 300 to 600 nm and 540 to 900 nm, as two different gratings were required due to the latter range requiring a filter. To account for the response of the lamp, the response of a silicon diode was tested as a normalization measurement. The photoresponse of the silicon diode was corrected using its known responsivity. The third measurement was determination of the photocurrent variation generated by direct interaction of x-ray photons with the device as a function of the accumulated dose.

The direct response to x rays was also characterized as a function of radiation damage by irradiation with x rays with an average energy of 70 keV and dose rate of 3.9 kGy/s. The OPD was irradiated in steps depositing 400 Gy per step, up to a total dose of 40 kGy. The response of the detector was recorded in real time using the XTREAM data acquisition system (DAS).[47] Uncertainties were determined by the standard variation of the intensity from the DAS due to the intrinsic noise of the response.

2.C. Response characterization

X-ray response measurements were performed using 6 MV x rays from a Varian Clinac 21iX linear accelerator (LINAC). The LINAC produced a pulsed radiation source with a pulse width of 3.6 μs and an instantaneous dose rate of 2.7×10^{-4} Gy/pulse at calibration conditions. At a nominal rate of 600 MU/min, the dose rate in reference conditions equals 6 Gy/min. The detectors were embedded within a $30 \times 30 \times 1$ cm^3 plexiglass holder and connected to a custom-designed electrometer for real-time collection of the instantaneous charge for all measurements.[48] Each scan was repeated three times to calculate an average and evaluate uncertainties as one standard deviation of the intensity. An external reverse bias of 2 V was applied across the OPD. Reference conditions for dosimetry in the 6-MV photon beam were a source to surface distance (SSD) of 100 cm, a field size of 10x10 cm^2 and sample depth of 1.5 cm, that is, d_{max} for 6-MV modality in a water equivalent plastic phantom, with an additional 10 cm of backscatter. The detector was composed of a scintillator and a photodiode which are both exposed to the same photon flux. In order to establish the signal induced by radiation interacting directly with the OPD, the device response was tested by exposing the samples to ionizing radiation in two modalities: by direct interaction (radiation interacts with OPD devices directly) and by indirect interaction (radiation is converted into optical photons within the scintillator). The plastic scintillator (RP400) had a peak emission wavelength of 420 nm. To minimize reflections at the surface the scintillator was coupled with the devices using optical grease with a refractive index of 1.457 to 1.466[49] which is close to that of the organic scintillators, 1.58,[50] and the OPD protective layer, 1.3.

2.C.1. Linearity

Dose linearity measurements were performed for 6-MV photons at reference conditions as previously described (1 MU = 1 cGy). The response was recorded from 25 to 100 cGy in 25 cGy increments then up to 500 cGy in

increments of 100 cGy. Photodetector sensitivity was calculated from the gradient of the linearity plot (nC/cGy).

2.C.2. Dose rate dependence

The response of the detector, relative to an ionization chamber (IC) (NE2571 Farmer) positioned in reference conditions, was tested under different irradiation dose rates by varying the SSD from 300 to 90 cm. This corresponds to a dose per pulse (DPP) range between 0.31×10^{-4} Gy/pulse and 3.4×10^{-4} Gy/pulse, respectively. Readings at each SSD were divided by the response of the IC and the ratios were normalized to the response ratio measured at an SSD of 100 cm, corresponding to a DPP of 0.28 mGy/pulse. Assuming that the IC response was dose rate independent in the range of interest, then normalizing the response of the OPD to this chamber at different SSDs provided a mechanism for determining the dose rate dependence of the OPD.

2.C.3. Energy dependence

For energy dependence measurements, the response of the OPD coupled with a plastic scintillator to 6-MV photons at reference conditions was compared to keV energies from a Gulmay orthovoltage x-ray tube. The x-ray tube operated at accelerating potentials between 50 and 250 kVp corresponding to incident mean photon energies of 29.5 and 129.4 keV. 100 MU was incident onto the OPDs at 30 and 50 cm focus skin distances (FSDs), depending on the applicator used for the desired energy. All measurements were conducted at the surface with 10cm backscatter of water equivalent plastic phantom.

2.C.4. Percentage depth dose

Percentage depth dose (PDD) measurements for pulsed 6-MV photons were obtained for the device in a water equivalent plastic phantom and compared to an IC (Scanditronix/Wellhofer CC13) in a water tank. With the SSD remaining constant, that is, 100 cm, the PDD was measured from 0.5 to 25 cm by stacking increasing thicknesses of water equivalent plastic phantom on top of the device, with a constant 10 cm backscatter. The PDD of the OPD was measured via direct detection (no scintillator) and indirect detection with plastic scintillators of different thicknesses (from 0.5 to 2 mm). The response of the OPD was compared to the response obtained using an IC.

3. RESULTS

3.A. Radiation hardness study

The results of the JV characterization performed between −10 and 2 V bias as a function of ionizing radiation dose are shown in Fig. 2. An inset highlights the effect on current density of accumulated dose at −2 V. This value of external bias was subsequently used as the operating voltage for all further experiments as it represents the minimum reverse bias value required to ensure complete charge extraction under operating conditions.

The effect of radiation damage to the OPDs ability to detect visible light is illustrated in Fig. 3. The maximum photocurrent for the nonirradiated device was obtained at a wavelength of 640 nm compared to 370 nm after 40 kGy. The change in spectral shape was due to the acceptor (absorbance peak at 370 nm) clearly withstanding the irradiation better than the polymer donor (broad 450 to 600 nm peak). The wavelength of maximum photocurrent was chosen for the scintillator to optimize the signal of the OPD after preirradiation.

The effect of irradiation by high-energy x rays on the photodiodes ability to directly detect ionizing radiation is illustrated in Fig. 4. The photodiodes had a response efficiency of approximately 30% after a cumulative irradiation dose of 30 kGy. At doses of 35 kGy or higher, the variation of any subsequent changes in charge output was observed to be <0.5%.

3.B. Response characterization

Response of the organic photodetector to a 6-MV photon beam was measured via direct interaction (without a scintillator) and indirect interaction (with a 0.5-mm-thick scintillator) as presented in Fig. 5. Direct interaction produced a low x-ray induced photocurrent with a poor signal-to-noise ratio (approximately (5 ± 1) pC of charge integrated over 1 ms) with respect to the signal generated by optical photons from the scintillator corresponding to a charge of (135 ± 1) pC. Response timing of the OPD to direct interaction with the x rays shows a different behavior with respect to the response

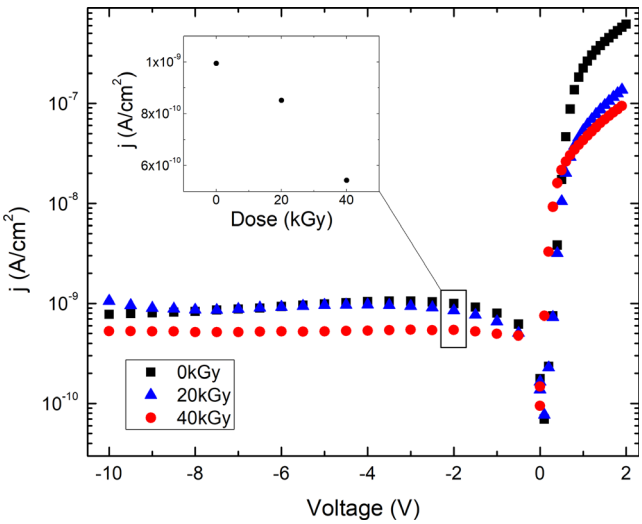

FIG. 2. JV characteristics for the organic photodetectors preirradiated to a total irradiation dose of 20 kGy (blue triangles) and 40 kGy (red circles) with respect to the reference sample (nonirradiated) (black squares). The inset shows the trend of the leakage current density at −2 V as a function of the accumulated dose.

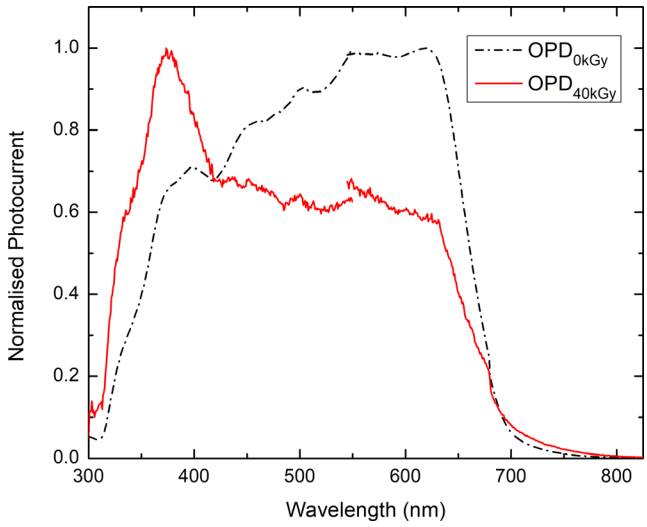

FIG. 3. Spectral response of the nonirradiated 0 kGy (black dash-dot line) and preirradiated 40 kGy (red solid line) organic photodetectors.

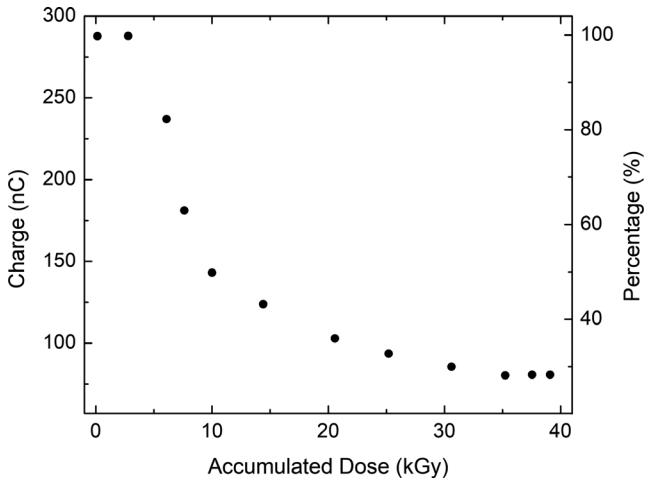

FIG. 4. Variation of the photodiode response as a function of total irradiated dose by irradiation with <E> = 70 keV x rays. Uncertainties were smaller than the marker size, on the order of ±5 pC.

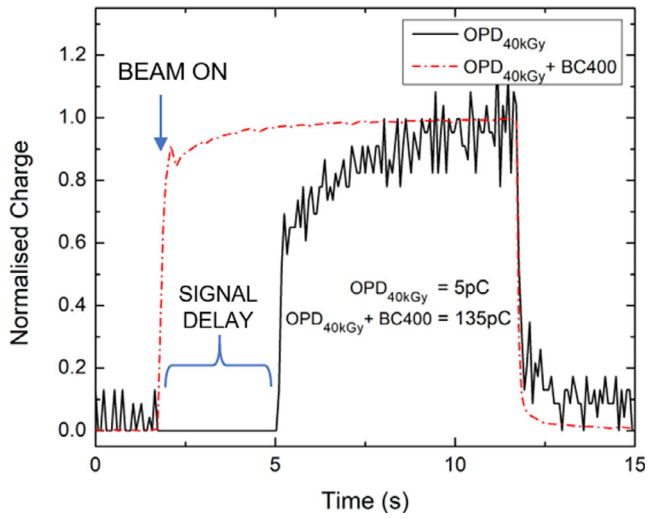

FIG. 5. Response of preirradiated organic photodiode to beam from pulsed LINAC for 100 MU in calibration conditions via direct (black solid line) and indirect (0.5-mm-thick RP400 plastic scintillator) (red dash-dot line) detection in passive mode. Waiting 5 min between prior exposure to 6-MV photons showed a delayed response between the beam turning on (blue arrow) and the response observed from direct detection.

generated by the optical photons emitted by the scintillator. The electrons generated directly in the OPD device by the x rays do not generate a conductive current for the first few seconds of irradiation. This effect, often referred to as the priming effect, has been observed in several different analogous radiation detectors, in particular for amorphous detectors such as polyCVD diamond devices.[51,52] The delayed current response is generally ascribed to carriers filling the traps of the low-energy tail states of the acceptor and donor materials. For the OPDs in this study, priming was required every time the detector was left un-irradiated (in dark conditions) for 5 min or more.

The responses of the OPDs to indirect detection of high-energy photons were observed to be linear from 25 to 500 Gy with an R^2 value of 0.9991 and 1 for the nonirradiated and preirradiated sample (Fig. 6), respectively. Their sensitivities to 6-MV photons were determined to be (190.0 ± 0.3) pC/cGy and (170 ± 0.10) pC/cGy at −2 V, respectively.

Figure 7 shows that, if the detector is equipped with the scintillator, the dose rate dependence is uniform and the indirect detection of ionizing radiation for organic semiconductors is constant, irrespective of the injection level and preirradiation conditions. The response of the OPD to direct interactions with secondary electrons at d_{max} (under 1.5 cm of solid water) is a factor of 2 higher at lower dose rates, before stabilizing at rates higher than 2×10^{-4} Gy/pulse. This dose rate dependence for direct detection was even higher for the preirradiated device, reaching a factor of 2.4.

The energy dependence was measured for a preirradiated organic photodiode for indirect detection (2-mm scintillator thickness) of low keV energies from an orthovoltage x-ray unit and compared to the response from pulsed 6-MV photons, as shown in Fig. 8. The gradient from 30 to 100 keV is due to the absorption properties of the plastic scintillator used. The mass-energy absorption coefficient ratio of the plastic scintillator to water provided by the National Institute of Standards and Technology (NIST)[2] in Fig. 8 proves this hypothesis. The uncertainty is strongly affected by the dose rate from the orthovoltage x-ray tubes at a specific energy due to the need for longer/shorter acquisition times to deposited 100 MU during each scan. The dose rates ranged from 9 to 42.5 mGy/s, occurring at 100 and 50 keV, respectively. However, as shown in Fig. 7, when coupled with a scintillator the device is not dose rate dependent, it is only the signal-to-noise ratio from the orthovoltage output that affects the uncertainty in Fig. 8. The energy offset observed between the NIST data and the experimental data from the detector is due to the use of a broad spectrum with a nominal average energy

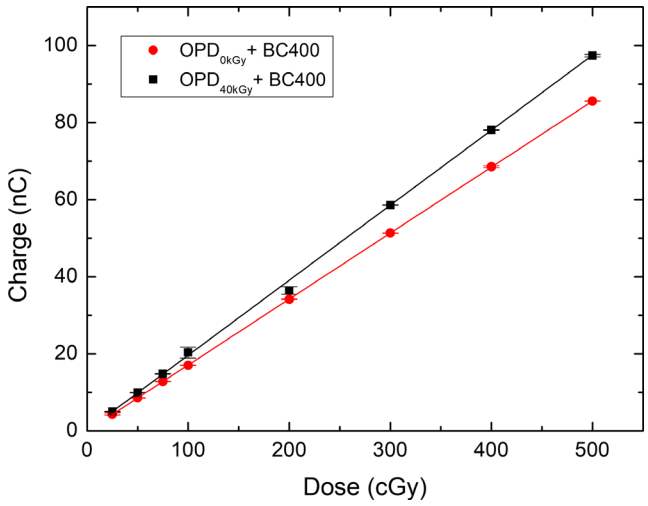

FIG. 6. Linear dose response of nonirradiated 0 kGy (black squares) and preirradiated 40 kGy (red circles) organic photodetectors from indirect detection (0.5-mm-thick RP400 plastic scintillator) of 6-MV photons at − 2 V external bias. The uncertainties were calculated as one standard deviation from three datasets.

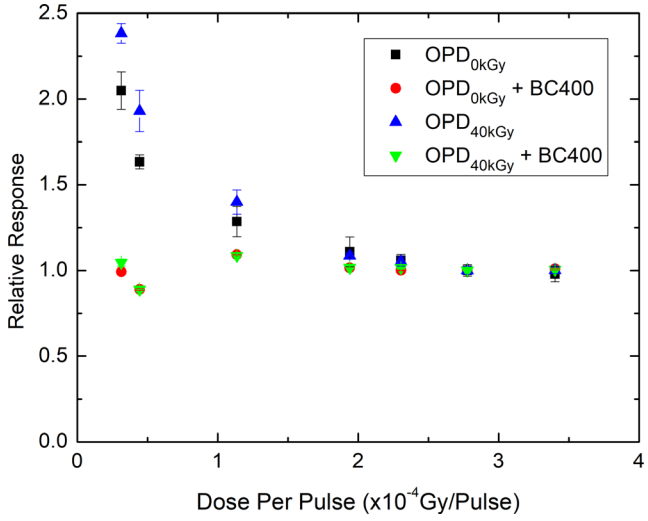

FIG. 7. Dose per pulse response of the nonirradiated 0 kGy (black squares and red circles) and preirradiated 40 kGy (blue up triangles and green down triangles) organic photodetectors. Measurements were obtained at dmax in a water equivalent solid phantom with a 6-MV photon beam at a field size of 10 × 10 cm^2, SSD from 90 to 300 cm and − 2 V external bias. Both direct (organic photodetector) and indirect (organic photodetector coupled with a 2-mm-thick RP400 plastic scintillator) detection are reported for comparison. The uncertainties were calculated as one standard deviation from three datasets.

for the experimental measurements while the absorption calculated by NIST is for a monochromatic source. Fig. 8 also compares the energy dependence for commercially available detectors as a reference.

A comparison of the PDD measured for the photodetector from the surface to 20 cm depth in solid water is presented in Fig. 9. All datasets were normalized to d_{max} for a 6-MV photon beam with 10 × 10 cm^2 field. Figure 9(a) illustrates the effect of the PDD using a range of plastic scintillator

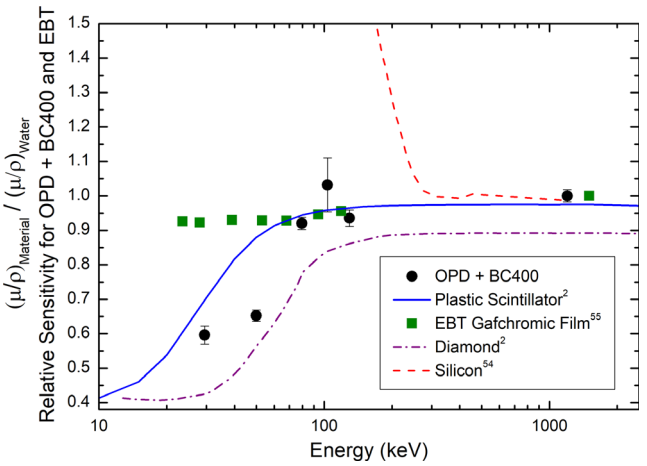

FIG. 8. Energy dependence characterized by the response of the preirradiated organic photodiode (black circles) by indirect detection (2-mm-thick RP400 plastic scintillator) of keV photons from an x-ray tube and 6-MV photon beam in comparison to the response of the plastic scintillator (blue solid line) and diamond (purple dash-dot line) data obtained from NIST, and silicon[60] (red dash line) and, film[61] (green squares) detectors.

thicknesses. The data collected with the 1-mm scintillator provide the most accurate match with respect to the IC data as demonstrated in Fig. 9(c). The percentage difference for the 1-mm scintillator with readout from the nonirradiated OPD was within ±3%, while the preirradiated device over responded by up to 5%. The inherent damage of the material due to the TID of 40 kGy has an impact on the ability of the device to accurately measure the dose deposited in direct comparison to an IC.

4. DISCUSSION

The radiation tolerance of organic semiconducting materials is a crucial parameter for design of a QA device for radiotherapy and must be proven to ensure that sensitive volume composites have a stable and reproducible response and a long shelf life for applications with high ionizing radiation exposure. JV characteristics of a device exposed to a TID of 20 kGy showed a decrease in the current rectification with an unchanged reverse bias leakage current (Figure 2). A decrease in the leakage current was observed for a TID of 40 kGy with an even further decrease in the rectification junction. This characterization suggests that an OPD can be used with a small bias applied because the baseline decreases with the exposure to radiation with a rate of approximately 0.01 fA/Gy. The JV characteristics suggest also that both lifetime and mobility of thermal carriers decrease. The effect of radiation damage on the OPD response has been characterized using both optical light and direct x-ray interaction (without a scintillator). Ionizing radiation induced trapping sites resulted in an overall decrease in sensitivity of the highly irradiated OPD which exhibited a shift in the maximum UV–Vis absorbance from 600 to 370 nm, substantially altering the spectral shape (Fig. 3). Since the photocurrent spectrum

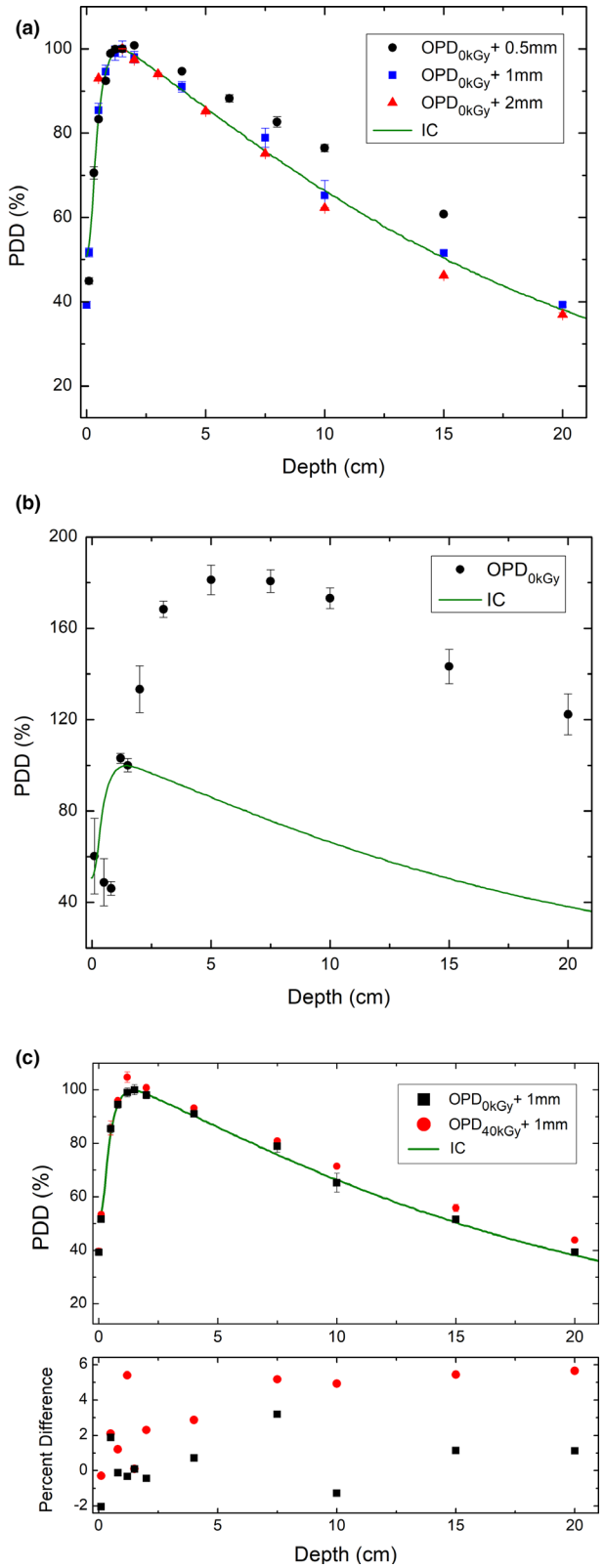

FIG. 9. Percentage depth dose (PDD) measured by an organic photodiode at 100 cm source to surface distance in a water equivalent solid phantom with comparison to an ionization chamber measurement by (a) indirect detection of different scintillator thicknesses and (b) direct detection. (c) Shows a comparison of the PDD with a scintillator thickness of 1mm coupled to the non- and preirradiated organic photodiode with the percentage difference to an ionization chamber.

is determined by the efficiency of current generation for each wavelength, it shows that radiation damage has a larger impact on the OPD in detecting long wavelengths than short. This result suggests that the polymer acceptor is more radiation tolerant compared to the polymer donor. Investigations of the effect that radiation damage has on their sensitivity to x rays, with an average energy of 70 keV, showed that the OPDs exhibit an acceptable response efficiency of approximately 30% after 35 kGy of irradiation (Fig. 4). Substantial degradation up to 1 kGy has been confirmed in other work[53] and is consistent with the morphological degradation expected for P3HT.[54] A stabilization of the response after 1 kGy is hypothesized to be a result of radiation induced conductivity (RIC). Radiation induced conductivity is a phenomenon observed in polymers irradiated with x rays from 20 to 400 keV. Photons generate free holes (as secondary electrons are promptly trapped) which undergo a rapid process of geminate generation and recombination, facilitating an increase in conductivity of the material.[55] This effect enhances the current signal collected at the electrode during irradiation and has been previously investigated in polymer materials. The RIC effect was found to be dependent on the electric field, temperature, and relative work function of the metal and organic substrate in these materials.[14,56] Thus, severe radiation damage with doses up to 30 kGy acts as a gettering effect, varying the fine structure of energy levels at the lowest unoccupied molecular orbital (LUMO) band, and improving the charge collection efficiency. We suggest that the mechanisms for the two charge transport processes differ such that exposure to high fields of ionizing radiation is only substantially affecting the photo generated charges via the absorption of visible photons. This hypothesis was formulated as a result of the substantial degradation of sensitivity when exposed to visible photons (Fig. 3) compared to the stabilizing effect for ionizing radiation (Fig. 4). The radiation damage effects were investigated for the response to 6-MV photons by comparison of a non- and preirradiated photodetector. All response and dosimetric measurements were conducted for a device consisting of an OPD coupled with a plastic scintillator emitting in the 400 to 420 nm range to take advantage of the response obtained from the UV–Vis photocurrent spectra. Coupling the organic photodiode with a plastic scintillator was also shown to produce higher sensitivity and a more stable response compared to direct detection (Fig. 5). The sensitivity to 6-MV photons when coupled with a 0.5-mm-thick scintillator was determined to be (190.0 ± 0.3) pC/cGy and (170 ± 0.10) pC/cGy for the nonirradiated and preirradiated sample at -2 V external bias, respectively, Fig. 6. The observed linear response of the OPDs when coupled with a plastic scintillator allowed for successful dosimetry measurements to be achieved before and after preirradiation. Differences in the response for direct and indirect detection were observed when measuring the dose rate dependence, Fig. 7. The response obtained with a scintillator across a large range of dose rates shows an excellent uniformity in comparison with a Farmer IC. The OPD without a scintillator instead shows a variation in the response

by a factor of approximately 2.5 before stabilizing past 2×10^{-4} Gy/pulse, suggesting that the exposure to high-energy photons changes the transport mechanism or the interaction of the carriers with the fine structure of the molecular orbitals in the substrate. Further studies of the carrier mobility and lifetime are required using pulsed x-ray sources to understand the mechanism of mobility underlying this effect.

The energy dependence of commercially used dosimeters is illustrated in Fig. 8. Silicon detectors have a characteristic over-response to photon energies below 0.2 MeV due to the larger cross section of the photoelectric effect of silicon ($Z = 14$) with respect to water. Film displays a weak energy dependence (within 10%) which is ideal for radiotherapy. Compared with these devices, the energy response of the OPDs when coupled with a plastic scintillator is dominated by the mass absorption coefficient of the scintillating material as shown by the match with the scintillator absorption data obtained from NIST. The detector exhibits an energy independent response within a wide range (between 70 keV and 1.2 MeV). This result shows that the organic semiconducting photodiode inherently has a minimal energy dependence of its response with the applicability to simultaneously measure x-ray beams of different energies for applications such as external beam radiotherapy and brachytherapy.[57–59]

The PDD was measured for a range of scintillator thicknesses as shown in Fig. 9(a). An over-response was observed for the thinnest scintillator compared to an underresponse for the thicker scintillator. The latter is due to a volume averaging effect with a sensitive volume thickness of 2 mm. The over-response occurring with the 0.5-–mm scintillator was due to the parasitic effect of the current generated in the OPD by direct interaction with the beam as shown by the direct correlation of the response of the OPD to a PDD curve shown in Fig. 9(b). The PDD as measured by the photodiode without a scintillator shows an unusual distribution of the dose. The PDD reached up to 180% between 5 and 7 cm depth because there is a combination of dose rate dependence (accountable for approximately 50% over-response) and a residual 30% dose enhancement which could be related to the extracameral materials around the OPD. This effect is measurable in the device without a scintillator because the current induced in the sensitive volume by the direct interaction with the beam is extremely small and luminescence and scattering from the printed circuit board underneath the sensor becomes a substantial portion of the total signal. This effect disappears when the OPD is coupled with the scintillator. Therefore, a 1-mm scintillator was observed to be the optimal thickness, as this sensitizer/detector combination minimized the volume averaging effect and created an intense optical signal to ensure that parasitic contributions from the OPD direct photocurrent and scattered radiation were negligible, Fig. 9(c).

Identifying the possible interactions of the organic semiconductor with ionizing radiation is still to be researched. An intensive investigation of the effect of radiation damage on the charge transport mechanism in organic semiconductor materials is not within the scope of this paper and is being examined with additional measurements. However, the variation in current response of <0.5% after an accumulated dose of 35 kGy demonstrates the possibility to stabilize the OPDs response to cumulative radiation dose. This result confirms that the response of an organic semiconductor device to ionizing radiation can be optimized for dosimetry in treatment and imaging applications. This study also showed that OPDs have the best response when coupled with a scintillator to measure the indirect detection of ionizing radiation. However, coupling with a plastic scintillator reduces the spatial resolution, increases the sensitive volume, and combines all the limitations of scintillators including isotropic emission, quantum efficiency of the scintillator and effects of coupling to the readout device.

5. CONCLUSIONS

This work presented investigations into the potential use of an organic photodetector coupled to a plastic scintillator as a dosimeter for ionizing radiation. The advantage of having a water equivalent material for both the sensitive volume (plastic scintillator) and the readout detector (photodiode) is attractive for dosimetry. The device can potentially combine the advantages of fiber-optic dosimeters and the simplicity of the readout of a diode. Radiation damage in organic semiconductors represents a limiting factor, which has been investigated in this work along with their performance as dosimeter. Both the samples, before and after irradiation, showed a linear response to accumulated dose. The nonirradiated organic photodetector performed slightly better, with a dose sensitivity of (190.0 ± 0.3) pC/cGy and a percentage difference of $\pm 3\%$ for the PDD between 0.5 and 20 cm, than the photodetector irradiated with 40 kGy of ionizing radiation. No dose rate dependence was observed for either photodetector, and energy dependence was shown to only affect the plastic scintillator coupled to the device. The comparison of the dose rate dependence and PDD for direct and indirect detection suggests that there is a differing transport mechanism within organic semiconducting material when excited by either visible light or ionizing photons. The signal generated by direct interaction of radiation with the photodiode is strongly dose rate dependent, which affects the response of the sensor to variation of the depth with respect to the ionization chamber. In order to achieve a reliable and accurate percentage depth dose curve, a minimum thickness of 1-mm scintillator must be used to make the direct interaction response of the photodiode negligible. The response of an organic photodiode to x rays can be stabilized with a variability of 0.5% after preirradiation with 30 kGy. This result confirms that the combination of an organic scintillator with an organic photodiode is a viable solution for tissue equivalent dosimetry, but investigation into correcting for the lower sensitivity and dose rate dependence for direct detection must be addressed. This could potentially be achieved by exploring different combinations of the bulk heterojunction materials and the thickness of the device.

ACKNOWLEDGMENTS

The authors thank the group at the University of Bologna for facilitating our research into the exploration of radiation damage in organic semiconductors and to the beamline staff at the Australian Synchrotron for access to the facilities. Also, to the Illawarra Cancer Care Centre for the use of their linear accelerator, orthovoltage unit and dosimetry equipment and ISORG for providing the devices. This work was supported by the Australian Government Research Training Program Scholarship, as well as the Australian Institute of Nuclear Science and Engineering Post-Graduate Research Award, and the University Global Partnership Network Research Collaboration Fund.

CONFLICT OF INTEREST

The authors have no conflict to disclose.

[a]Author to whom correspondence should be addressed. Electronic mail: marcop@uow.edu.au.

REFERENCES

1. Andreo P. The physics of small megavoltage photon beam dosimetry. *Radiother Oncol*. 2018;126:205–213.
2. Hubbell JH, Seltzer SM. X-Ray Mass Attenuation Coefficients. National Institute of Standards and Technology NIST Standard Reference Database 126. https://www.nist.gov/pml/x-ray-mass-attenuation-coefficients. Published 2004. Accessed September 20, 2019.
3. Berger MJ, Coursey JS, Zucker MA, Chang J. Stopping-Power & Range Tables for Electrons, Protons, and Helium Ions. National Institute of Standards and Technology NIST Standard Reference Database 124. https://www.nist.gov/pml/stopping-power-range-tables-electrons-protons-and-helium-ions
4. Peter B, Tommy K, Per N. Comparative dosimetry of diode and diamond detectors in electron beams for intraoperative radiation therapy. *Med Phys*. 2000;27:2580–2588.
5. Bauer C, Baumann I, Colledani C, et al. Radiation hardness studies of CVD diamond detectors. *Nucl Inst Methods Phys Res A*. 1995;367:207–211.
6. Laub W, Crilly R. Clinical radiation therapy measurements with a new commerical synthetic single crystal diamond detector. *Med Phys*. 2014;15:92–102.
7. Davis JA, Guatelli S, Petasecca M, et al. Tissue equivalence study of a novel diamond-based microdosimeter for galactic cosmic rays and solar particle events. *IEEE Trans Nucl Sci*. 2014;61:1544–1551.
8. Davis JA, Lazarakis P, Vohradsky J, et al. Tissue equivalence of diamond for heavy charged particles. *Radiat Meas*. 2019;122:1–9.
9. Kashiwagi T, Hibino K, Kitamura H, et al. Investigation of basic characteristics of synthetic diamond radiation detectors. *IEEE Trans Nucl Sci*. 2006;53:630–635.
10. Girolami M, Bellucci A, Calvani P, et al. Large single-crystal diamond substrates for ionizing radiation detection. *Physica Status Solidi (a)*. 2016;213:2634–2640.
11. Girolami M, Bellucci A, Calvani P, et al. Mosaic diamond detectors for fast neutrons and large ionizing radiation fields. *Phys Status Solidi Appl Mater Sci*. 2015;212:2424–2430.
12. Butler DJ, Beveridge T, Lehmann J, Oliver CP, Stevenson AW, Livingstone J. Spatial response of synthetic microDiamond and diode detectors measured with kilovoltage synchrotron radiation. *Med Phys*. 2018;45:943–952.
13. Livingstone J, Stevenson AW, Butler DJ, Häusermann D, Adam JF. Characterization of a synthetic single crystal diamond detector for dosimetry in spatially fractionated synchrotron x-ray fields. *Med Phys*. 2016;43:4283–4293.
14. Fournier P, Cornelius I, Dipuglia A, et al. X-Tream dosimetry of highly brilliant X-ray microbeams in the MRT hutch of the Australian synchrotron. *Radiat Meas*. 2017;106:405–411.
15. Looe HK, Poppinga D, Kranzer R, et al. The role of radiation-induced charge imbalance on the dose-response of a commercial synthetic diamond detector in small field dosimetry. *Med Phys*. 2019;46:2752–2759.
16. Podgorsak EB. *Radiation Oncology Physics: A Handbook for Teachers and Students*. Vienna: International Atomic Energy Agency; 2005.
17. Richley L, John AC, Coomber H, Fletcher S. Evaluation and optimization of the new EBT2 radiochromic film dosimetry system for patient dose verification in radiotherapy. *Phys Med Biol*. 2010;55:2601–2617.
18. Li Y, Chen L, Zhu J, Liu X. The combination of the error correction methods of GAFCHROMIC EBT3 film. *PLoS ONE*. 2017;12:e0181958.
19. Martišíková M, Ackermann B, Jäkel O. Analysis of uncertainties in Gafchromic® EBT film dosimetry of photon beams. *Phys Med Biol*. 2008;53:7013–7027.
20. Baldock C, De Deene Y, Doran S, et al. Topical review: polymer gel dosimetry. *Phys Med Biol*. 2010;55:R1–R63.
21. Beddar S, Beaulieu L. *Scintillation Dosimetry*. Boca Raton: CRC Press; 2016.
22. Archer J, Li E, Davis J, Cameron M, Rosenfeld A, Lerch M. High spatial resolution scintillator dosimetry of synchrotron microbeams. *Sci Rep*. 2019;9:6873.
23. Knoll GF. *Radiation Detection and Measurement*, 4th edn. New York: Wiley; 2010.
24. Archer J, Li E, Petasecca M, et al. X-ray microbeam measurements with a high resolution scintillator fibre-optic dosimeter. *Sci Rep*. 2017;7:1–7.
25. Clift MA, Sutton RA, Webb DV. Dealing with Cerenkov radiation generated in organic scintillator dosimeters by bremsstrahlung beams. *Phys Med Biol*. 2000;45:1165–1182.
26. Beddar AS, Mackie TR, Attix FH. Cerenkov light generated in optical fibres and other light pipes irradiated by electron beams. *Phys Med Biol*. 1992;37:925–935.
27. Griffith MJ, Cottam S, Stamenkovich J, Posar JA, Petasecca M. Printable organic semiconductors for radiation detection: from fundamentals to fabrication and functionality. *Front Phys*. 2020;8:1–21.
28. Anderson D, Cottam S, Heim H, Zhang H, Holmes NP, Griffith MJ. Printable ionizing radiation sensors fabricated from nanoparticulate blends of organic scintillators and polymer semiconductors. *MRS Commun*. 2019;9:1206–1213.
29. Griffith MJ, Holmes NP, Elkington DC, et al. Manipulating nanoscale structure to control functionality in printed organic photovoltaic, transistor and bioelectronic devices. *Nanotechnology*. 2020;31:092002.
30. Kingsley JW, Weston SJ, Lidzey DG. Stability of x-ray detectors based on organic photovoltaic devices. *IEEE J Sel Top Quantum Electron*. 2010;16:1770–1775.
31. Shirota Y, Kageyama H. Charge Carrier Transporting Molecular Materials and Their Applications in Devices. *Chemical Reviews*. 2007;107:953–1010. http://dx.doi.org/10.1021/cr050143+.
32. Yoshino K, Hayashi S, Ishii G, Inuishi Y. Electrical transport in electron beam irradiated polyacetylene. *Solid State Commun*. 1983;46:405–408.
33. Beckerle P, Ströbele H. Charged particle detection in organic semiconductors. *Nucl Instruments Methods Phys Res Sect A Accel Spectrometers, Detect Assoc Equip*. 2000;449:302–310.
34. Mills CA, Intaniwet A, Shkunov M, Keddie JL, Sellin PJ. Flexible radiation dosimeters incorporating semiconducting polymer thick films. 2009;7449:74491I. https://doi.org/10.1117/12.829619
35. Boroumand FA, Zhu M, Dalton AB, Keddie JL, Sellin PJ, Gutierrez JJ. Direct x-ray detection with conjugated polymer devices. *Appl Phys Lett*. 2007;91:3–6.
36. Intaniwet A, Keddie JL, Shkunov M, Sellin PJ. High charge-carrier mobilities in blends of poly(triarylamine) and TIPS-pentacene leading to better performing X-ray sensors. *Org Electron Phys Mater Appl*. 2011;12:1903–1908.
37. Mills CA, Al-Otaibi H, Intaniwet A, et al. Enhanced x-ray detection sensitivity in semiconducting polymer diodes containing metallic nanoparticles. *J Phys D Appl Phys*. 2013;46:275102.

38. Ciavatti A, Cramer T, Carroli M, et al. Dynamics of direct X-ray detection processes in high-Z Bi2O3nanoparticles-loaded PFO polymer-based diodes. *Appl Phys Lett*. 2017;111:183301.
39. Thirimanne HM, Jayawardena KDGI, Parnell AJ, et al. High sensitivity organic inorganic hybrid X-ray detectors with direct transduction and broadband response. *Nat Commun*. 2018;9:2926.
40. Kohler A, Bassler H. *Electronic Processes in Organic Semiconductors: An Introduction*. Weinheim: Wiley-VCH Verlag GmbH & Co. KGaA.; 2015.
41. Thompson BC, Fréchet JMJ. Polymer-fullerene composite solar cells. *Angew Chem Int Ed*. 2008;47:58–77.
42. Devine RAB, Mayberry C, Kumar A, Yang Y. Origin of radiation induced damage in organic P3HT:PCBM based photocells. *IEEE Trans Nucl Sci*. 2010;3109–3113.
43. Keivanidis PE, Greenham NC, Sirringhaus H, et al. X-ray stability and response of polymeric photodiodes for imaging applications. *Appl Phys Lett*. 2008;92:1–3.
44. Kingsley JW, Pearson AJ, Harris L, Weston SJ, Lidzey D. Detecting 6 MV X-rays using an organic photovoltaic device. *Org Electron*. 2009;42:950–966.
45. Protopopov YM, Vasil'chenko VG. Radiation damage in plastic scintillators and optical fibers. *Nucl Inst Methods Phys Res B*. 1995;95:496–500.
46. Dettmann M, Herrig V, Maldonis J, et al. Radiation hard plastic scintillators for a new generation of particle detectors. *J Instrum*. 2017;12: P03017.
47. Petasecca M, Cullen A, Fuduli I, et al. X-Tream: a novel dosimetry system for synchrotron microbeam radiation therapy. *J Instrum*. 2012;7: P07022.
48. Fuduli I, Newall MK, Espinoza AA, et al. Multichannel data acquisition system comparison for quality assurance in external beam radiation therapy. *Radiat Meas*. 2014;71:338–341.
49. Scintillator Products. Rexon Components & TLD Systems, Inc. https://www.rexon.com/Accessories.htm. Published 2001. Accessed April 20, 2019.
50. Plastic Scintillator RP-400. Rexon Components & TLD Systems, Inc. https://www.rexon.com/RP400.htm. Published 2004. Accessed April 20, 2019.
51. Manfredotti C. CVD diamond detectors for nuclear and dosimetric applications. *Diam Relat Mater*. 2005;14:531–540.
52. Whitehead AJ, Airey R, Buttar CM, et al. CVD diamond for medical dosimetry applications. *Nucl Instrum Methods Phys Res Sect A Accel Spectrom Detect Assoc Equip*. 2001;460:20–26.
53. de Bettignies R, Leroy J, Chambon S, et al. Lifetime analysis and degradation study of polymer solar cells. *Org Optoelectron Photonics*. 2004;2004:122.
54. Leijten ZJWA, Keizer ADA, De With G, Friedrich H. Quantitative analysis of electron beam damage in organic thin films. *J Phys Chem C*. 2017;121:10552–10561.
55. Wojcik M, Nowak A, Seki K. Geminate electron-hole recombination in organic photovoltaic cells. A semi-empirical theory. *J Chem Phys*. 2017;146:054101.
56. Intaniwet A, Mills CA, Sellin PJ, Shkunov M, Keddie JL. Achieving a stable time response in polymeric radiation sensors under charge injection by X-rays. *ACS Appl Mater Interfaces*. 2010;2:1692–1699.
57. Wong JHD, Knittel T, Downes S, et al. The use of a silicon strip detector dose magnifying glass in stereotactic radiotherapy QA and dosimetry. *Med Phys*. 2011;38:1226–1238.
58. Petasecca M, Newall MK, Booth JT, et al. MagicPlate-512: a 2D silicon detector array for quality assurance of stereotactic motion adaptive radiotherapy. *Med Phys*. 2015;42:2992–3004.
59. Espinoza A, Beeksma B, Petasecca M, et al. The feasibility study and characterization of a two-dimensional diode array in 'magic phantom' for high dose rate brachytherapy quality assurance. *Med Phys*. 2013;40:111702–111710.
60. Rogers DWO, Cygler JE. Clinical dosimetry measurements in radiotherapy; Appendix A. Madison: *Med Phys*. 2009.
61. Butson MJ, Cheung T, Yu PKN. Weak energy dependence of EBT gafchromic film dose response in the 50 kVp-10 MVp X-ray range. *Appl Radiat Isot*. 2006;64:60–62.